



1,2,3-Triazolyl-4-oxoquinolines: A feasible beginning for promising chemical structures to inhibit oseltamivir-resistant influenza A and B viruses



Fernanda da C. S. Boechat^{a,†}, Carolina Q. Sacramento^{b,c,d,†}, Anna C. Cunha^a, Fernanda S. Sagrillo^a, Christiane M. Nogueira^a, Natalia Fintelman-Rodrigues^{b,c,d}, Osvaldo Santos-Filho^b, Cecília S. Riscado^a, Luana da S. M. Forezi^a, Letícia V. Faro^a, Leonardo Brozeguini^a, Isakelly P. Marques^a, Vitor F. Ferreira^a, Thiago Moreno L. Souza^{b,c,d,*}, Maria Cecília B. V. de Souza^{a,*}

^a Universidade Federal Fluminense, Instituto de Química—Outeiro de São João Batista, s/n°. Campus do Valonguinho, Centro, Niterói, RJ CEP 24020-150, Brazil

^b Fundação Oswaldo Cruz, Instituto Oswaldo Cruz, Laboratório de Vírus Respiratórios, NIC-WHO, Rio de Janeiro, RJ CEP 21041-360, Brazil

^c Fundação Oswaldo Cruz, Instituto Oswaldo Cruz, Laboratório de Imunofarmacologia, Rio de Janeiro, RJ CEP 21041-360, Brazil

^d Fundação Oswaldo Cruz, Centro de Desenvolvimento Tecnológico em Saúde, Rio de Janeiro, RJ CEP 21041-360, Brazil

ARTICLE INFO

Article history:

Received 11 September 2015

Revised 11 November 2015

Accepted 21 November 2015

Available online 26 November 2015

Keywords:

1,2,3-Triazole

4-Oxoquinoline

Influenza viruses

Neuraminidase inhibitors

Oseltamivir carboxylate

Antiviral resistance

ABSTRACT

We described the synthesis of a new congener series of 1,2,3-triazolyl-4-oxoquinolines and evaluated their ability to inhibit oseltamivir (OST)-resistant influenza strains. Oxoquinoline derivative **1i** was the most potent compound within this series, inhibiting 94% of wild-type (WT) influenza neuraminidase (NA) activity. Compound **1i** inhibited influenza virus replication with an EC₅₀ of 0.2 μM with less cytotoxicity than OST, and also inhibited different OST-resistant NAs. These results suggest that 1,2,3-triazolyl-4-oxoquinolines represent promising lead molecules for further anti-influenza drug design.

Published by Elsevier Ltd.

1. Introduction

Acute respiratory infections have a great impact on public health because they are a major cause of morbidity and mortality.¹ Influenza virus, a negative-sense-RNA orthomixovirus,² is the most important etiologic agent of severe acute respiratory infections (SARI). Influenza virus causes both seasonal infections and pandemic outbreaks.³ To enter host cells, influenza binds to sialic acid residues on glycoproteins localized in the cellular plasma membrane. This is followed by endocytosis and the fusion of the viral envelope with the endocytic membrane in a manner that is dependent on the viral protein M2.⁴ Next, viral ribonucleoproteins (RNP) composed of the RNA polymerase complex, viral RNA, nucleoprotein (NP) and nuclear export proteins (NEP) are released into the cytoplasm and transported to the cell nucleus, where transcription

and replication of the viral genome occur. Then, viral proteins are trafficked to the host cell plasma membrane for the assembly of new viruses. These particles bud through the cellular plasma membrane and are released via viral neuraminidase (NA) activity.⁵

Strategies to control influenza virus infections include vaccination and antiviral drugs.^{6,7} The existence of multiple zoonotic hosts,⁸ the time required to produce vaccines against novel viruses, the costs of vaccine production and its recommendation only for groups of patients at high risk for serious influenza-related illnesses represent major limitations for the use of vaccines.⁹ In contrast, anti-influenza drugs are now recommended for clinical use whenever possible because the most effective time frame for treatment is approximately 2.5 days after the onset of illness.¹⁰ Moreover, because the antigenic characteristics of viral strains that might cause future pandemic outbreaks are unpredictable, the stockpiling of anti-influenza drugs is a key issue in pandemic preparedness.^{11,12}

Virtually all circulating strains of influenza are resistant to the adamantanes (M2-channel blockers). Thus, neuraminidase inhibitors (NAIs) such as oseltamivir (OST), zanamivir, peramivir and

* Corresponding authors. Tel.: +55 21 26292148.

E-mail address: mceciliabvs@gmail.com (M.C.B.V. de Souza).

† These authors contributed equally as first authors.

‡ These authors contributed equally as last authors.

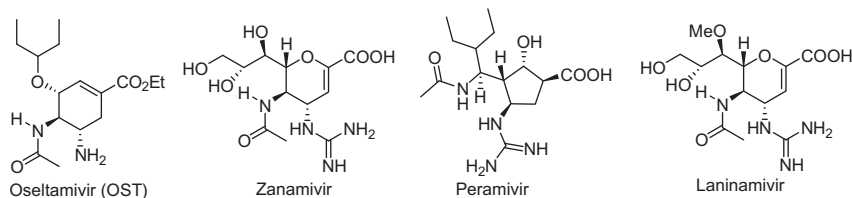


Figure 1. Structures of neuraminidase inhibitors (NAIs) approved for clinical use.

laninamivir constitute the only licensed class of drugs available for clinical use against influenza (Fig. 1).¹³ OST is the most used anti-influenza drug because it is orally administered and is licensed to more countries than the other drugs.¹⁴ However, approximately 1–2% of the circulating strains of influenza A(H1N1)pdm09 virus are resistant to OST, and OST-resistant viruses may also cause primary infections.^{15,16} Therefore, the identification of novel molecules endowed with the ability to inhibit OST-resistant strains of influenza is pivotal because it may increase the number of options available to fight this virus infection in the future.

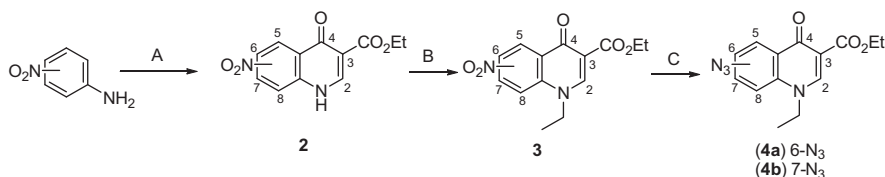
Quinolones and triazolic derivatives have been largely explored due to multiple biological properties. With respect to these radicals as antivirals, they have been proven to be active against HIV,^{17,18} HSV,¹⁹ HCV^{20,21} and influenza.^{22,23}

In this work, we synthesized new 4-oxoquinoline derivatives **1a–j** in which the core quinolone was connected to a 1,2,3-triazole nucleus and investigated their ability to inhibit influenza virus replication and the NA activity of OST-resistant strains of influenza. Importantly, our most effective compound inhibited multi-resistant strains of influenza. The triazolic ring and the cyclohexenyl radical were found to be critical for anti-influenza activity and allowed the compound to bind to conserved amino acid residues of both WT and OST-resistant NAs. Our results suggest that the chemical structure of 1,2,3-triazolyl-4-oxoquinolines is promising for the development of novel anti-influenza drugs.

2. Chemistry

The synthesis of 1,2,3-triazolyl-4-oxoquinoline derivatives **1a–j** was initiated with the treatment of *meta*- or *para*-nitroaniline with diethyl ethoxymethylenemalonate (EMME) to obtain enamine-type derivatives that were then cyclized in refluxing diphenyl ether.¹⁹

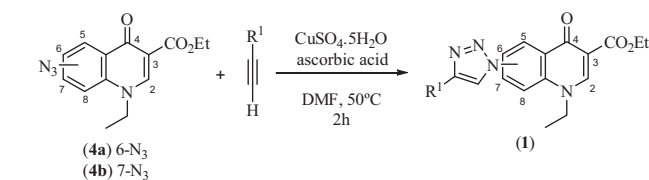
The corresponding 1,4-dihydro-4-oxo-quinolines **2** were submitted to an alkylation reaction with ethyl bromide, thereby affording the desired *N*-ethyl 4-oxoquinolines **3**.²⁴ After the chemical reduction of these compounds with iron and aqueous ammonium chloride solution, the diazonium salts of the amino-4-oxoquinolines were reacted with sodium azide, leading to desired azidoquinolones **4a–b** in quantitative yield (Scheme 1).²⁵ The azido-4-oxoquinolones **2a** and **2b** allowed us to study their application in the Huisgen ‘click-chemistry’ reaction using copper sulfate and ascorbic acid as the catalysts and dimethylformamide as the solvent at 50 °C²⁵ (Table 1).



Scheme 1. General synthetic route to obtain azidoquinolones **4a–b**: (A) (1) EMME, EtOH, reflux, 24 h; (2) diphenyl ether, 250 °C, 6 h; (B) K₂CO₃, DMF, EtBr, 80 °C, 24 h; (C) (1) iron, NH₄Cl 0.05 M; (2) NaNO₂, HCl, 30 min; (3) NaN₃, 15 min.

Table 1

Scheme summarizing the synthesis of 4-oxoquinoline **1a–j** moiety, R¹ substituents coupled to triazole ring located in positions C-6 or C-7 of the 4-oxoquinolines, the yield of each derivative after purification and their anti-influenza NA activity



#	R ¹	Triazole position	Yield (%)	Influenza H3N2 NA inhibition at 50 μM (%)
1a		C-6	88	59.1 ± 3.2
1b		C-7	85	62.3 ± 1.1
1c		C-6	83	56.5 ± 1.4
1d		C-7	79	57.4 ± 2.2
1e		C-6	97	89.0 ± 1.2
1f		C-7	93	56.3 ± 3.3
1g		C-6	95	0
1h		C-7	90	0
1i		C-6	98	94.8 ± 2.1
1j		C-7	95	44.5 ± 2.3

Their reactions with different alkynes resulted in the coupled inedited 4-oxoquinolines **1a–j**, with 79–98% yields after purification (Table 1).

All the structures of the new compounds **1a–j** were confirmed by spectral data (¹H and ¹³C NMR spectra) and by high resolution mass spectrometry analysis.

3. Results and discussion

3.1. Anti-influenza NA activity of 1,2,3-triazolyl-4-oxoquinoline derivatives

As mentioned above, NAIs are the only class of anti-influenza drug in clinical use. Although this class is effective against all NA types, drug-resistant influenza viruses have been described.^{15,16}

We initially performed NA inhibition assays with a single dose of 320 triazolic compounds. The molecules were tested against different NA types (or isoforms), either WT or OST-resistant enzymes. Ideally, high values for the ratio between the inhibitory activities against the OST-resistant and WT enzymes would indicate promising hits. We identified 8 promising compounds with ratios above 0.8. Among these, two 1,2,3-triazolyl-4-oxoquinoline derivatives showed ratios above 1.0 (Table S1), suggesting that they are more effective against the OST-resistant NA than the WT. Therefore, in this work we will further examine the mechanism of inhibition of these 1,2,3-triazolyl-4-oxoquinoline derivatives (hits 3 and 6 from Table S1), while the other hits will be studied in future works. All 1,2,3-triazolyl-4-oxoquinoline derivatives analyzed in this study are shown in Table 1 and named henceforth as compounds **1a–j**. Compounds **1e** and **1i** were the most potent against the NA activity, reaching inhibitions equal to 89.0% and 94.8%, respectively (Table 1).

For comparison, OST inhibits the NA activity at the same concentration of the tested compounds by 100%. Interestingly, **1e** and **1i** have similar R¹ substituents including a phenyl or cyclohexenyl ring, respectively; which is bound to the triazolic moiety at carbon 6 on the 4-oxoquinoline ring (Table 1). The change of the triazolic moiety position compromised the anti-influenza activity, probably because it interferes with the pattern by which our compound interacts with its targets. More interestingly, changes in R¹ radical, which led to a decrease in the steric space occupied by our compounds, could even abolish their anti-influenza activity (Table 1). Considering that these compounds are very similar, being molecule **1i** is slightly more potent than **1e**, subsequent experiments were performed with the former compound.

3.2. Potency of 1,2,3-triazolyl-4-oxoquinoline derivative **1i** against NA

To evaluate the potency of compound **1i**, we measured its ability to inhibit WT and OST-resistant NAs from circulating strains of influenza A and B. We can see, Table 2, that compound **1i** showed some advantages over OST in the inhibition of resistant strains of influenza. Although OST was more potent than compound **1i** in the inhibition of WT strains, compound **1i** IC₅₀ values suffered only marginal changes in the presence of resistance mutations to OST (Table 2). That is, the ratios of **1i**'s IC₅₀ values for OST-resistant NAs over the WT counterparts were 3.0, 0.13 and 1.4 for influenza A(H1N1)pdm09, A/H3N2 and B, respectively (Table 2). This indicates a marginal effect of OST-related resistance mutations towards compound **1i**'s ability to inhibit influenza A and B NAs (Table 2). The reference compound, OST, inhibited the NA activity of the antiviral resistant mutants of Influenza A(H1N1) [H275Y], A(H3N2) [E119V] and B [R152K] with higher IC₅₀ values when compared to WT enzymes, these values increased by 27-, 380- and 5.3-fold, respectively (Table 2). Therefore, our data indicate that compound **1i** chemical structure may be a promising

one to develop novel broad spectrum anti-influenza compounds able to impair the NA activity of OST-resistant strains.

3.3. Insights into the docking site of compound **1i** and its pharmacophore group

We showed above that the presence of the phenyl or cyclohexenyl ring linked to triazolic moiety bound to carbon C-6 of the 4-oxoquinoline derivatives was critical to inhibit influenza NA activity (Table 1) and compound **1i** (cyclohexenyl substituent) was able to inhibit OST-resistant influenza A and B NAs (Table 2). Thus, we next performed in silico docking studies of compound **1i** with WT and OST-resistant NAs (Table S2) to get insight on the pharmacophore group of this molecule and its predicted binding sites. Compound **1i** docked in the active site cleft of all tested isoforms of NA, either WT or resistant to OST (Fig. 2). The docking sites of compound **1i** and OST partially overlapped (Fig. 2A). The cyclohexenyl substituent shown above to be critical for the anti-influenza activity had a singular projection towards an area of the NA not occupied by OST (Fig. 2A and B), suggesting a possible mechanism on the inhibition of OST-resistant strains. Fig. 1C–G reveal multiple points of interaction between our compound and the amino acids in the active site of the NA. Moreover, the critical groups for biological activity (i.e., the triazolic moiety at position 6 and the cyclohexenyl ring) were nestled by very conserved amino acid residues among various influenza NA types (Figs. 2C–G and S1). These conserved amino acid residues are found in influenza viruses infecting either humans or animals (Figs. 2 and S1).²⁶ Because the pharmacophore group of compound **1i** docked in conserved areas of the NA in versatile ways, it is difficult to elicit specific amino acids to perform site-directed mutagenesis assays to further evaluate the particular contribution of amino acid residues to the interaction between compound **1i** and the influenza A and B NAs. Nevertheless, subsequent passages of the influenza virus in the presence of the compound **1i** are ongoing to evaluate whether influenza mutants resistant to compound **1i** may emerge.

For comparisons, all the interactions of compound **1i** and OST with their targets are displayed in Table 3. Compound **1i** bound to the different NAs with free energies comparable to those observed for OST (Table 3). Nevertheless, compound **1i** is endowed with the ability to inhibit isoforms of NA that OST binds without achieving any antiviral effects (Table 2).

OST interacts with the different NAs using more hydrogen bonds than compound **1i** (Table 3). However, compound **1i** was more versatile in interacting with the different NAs than OST, as judged by multiple steric hindrances with different amino acids residues (Table 3). Altogether, our data suggest that the 4-oxoquinolines moiety is important for compound **1i** docking, while the triazole ring and the cyclohexenyl radical are required for antiviral activity. It is important to note that our computational prediction (Table 3) revealed that OST interacted with the NAs as described in the literature.^{27,28}

3.4. Potency of compound **1i** against influenza replication and its cytotoxicity

Next, we evaluated the anti-influenza activity and cytotoxicity of compound **1i** cell-based assays. The EC₅₀ for compounds **1i** was 0.2 ± 0.01 μM, while for OST it was 0.03 ± 0.0023 μM (Table 4). Compound **1i** was less cytotoxic than OST, CC₅₀ values of 566 ± 89.5 μM and 321 ± 26 μM, respectively, were obtained (Table 4). Selective index (SI) values were calculated based on the ratio between the CC₅₀ and the EC₅₀ values. SI values for OST and compound **1i** were 10,700 and 2830, respectively (Table 4). Although OST' SI value is higher than the one observed for compound **1i**, our molecule is still very safe to be used in vitro. For

Table 2
Potency of the compound **1i** and the reference compound OST on WT and OST-resistant influenza strains

Influenza strains	IC ₅₀		IC ₅₀ change (times)	
	1i (μM)	OST (nM)	1i	OST
A/H3N2 WT	19.90 ± 1.3	0.15 ± 0.032	NA	NA
A/H3N2 E119V	2.60 ± 0.8	4.19 ± 0.16	0.13	27.00
A/H1N1 WT	3.50 ± 0.9	0.21 ± 0.011	NA	NA
A/H1N1 H275Y	10.60 ± 0.9	79.94 ± 3.2	3.00	380.00
B WT	22.00 ± 1.1	16.00 ± 2.9	NA	NA
B R152 K	30.00 ± 1.6	85.00 ± 5.4	1.40	5.30

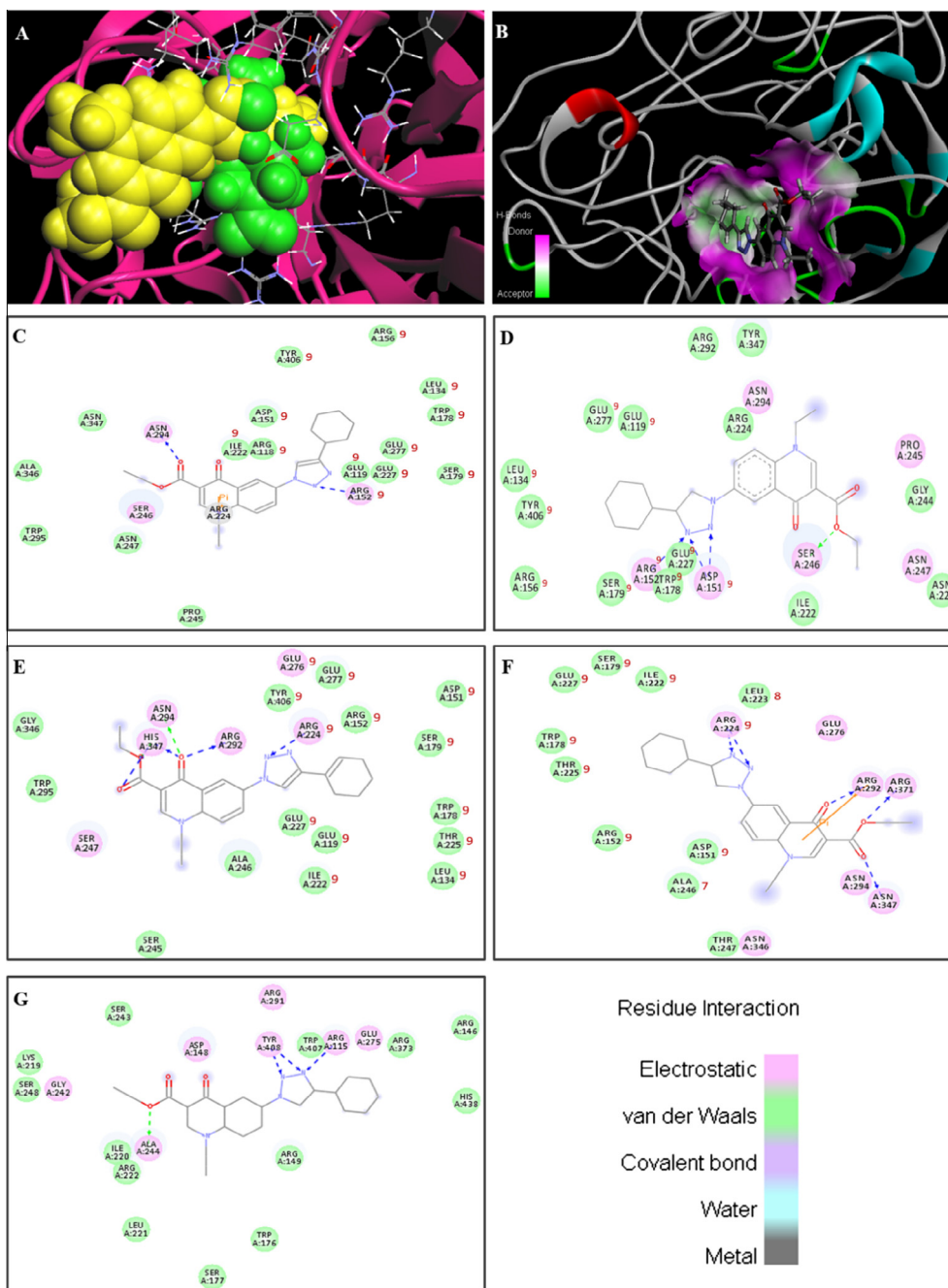


Figure 2. In silico analysis of compound **1i** bound to different isoforms of influenza NA enzyme. The crystal structure of WT N1 isoform with the compound **1i** (yellow) and OST (green) docked in the active site cleft (A). The cyclohexenyl radical of compound **1i** is projected to an area of NA enzyme which is not occupied by OST (B). 2D schematic figures showing compound **1i** docking to different NA isoforms are displayed as following: WT N1 (C), OST-resistant N1 (D), WT N2 (E), OST-resistant N2 (F) and WT influenza B NA (G). The types of interaction between compound **1i** and the NAs are indicated, hydrogen bounds are represented by dotted lines. The red numbers, next the amino acid residues surrounding the triazol ring and the cyclohexenyl moiety, represent in how many different types of influenza NA these residues are conserved (please see also Fig. S1).

comparisons, compound **1i** was more potent than other triazol derivatives described in the literature using cell-based assays, including the zanamivir analogues.²² These results indicate that compound **1i** is endowed with a very important margin between anti-influenza activity and cytotoxicity. These information, together with the anti-influenza activity over OST-resistant strains and the apparent ability to bind into conserved amino acid residues on NA, indicate that the chemical structure of compound **1i** is promising and may be of interest for further development of novel anti-influenza drugs.

4. Conclusions

Novel 4-oxoquinoline derivatives containing 1,2,3-triazolyl substituents **1a–j** were successfully synthesized and fully characterized. Compounds **1e** and **1i** were the most potent in inhibiting influenza virus NA enzymes. In addition to the inhibition of susceptible strains of influenza A and B, they also inhibited OST-resistant strains. Compound **1i** binds to the cleft of the active site in all WT and OST-resistant NA isoforms. The cyclohexenyl radical projects into an area of the NA that is not occupied by OST and is critical

Table 3
Compound **1i** and OST with WT and OST interactions during docking

Neuraminidase types	Compound 1i					OST				
	Binding energy (kcal/mol)	No. of hydrogen bonds	Amino acid residues involved in H-bonding	No. of bumps	Amino acid residues involved in bumps	Binding energy (kcal/mol)	No. of hydrogen bonds	Amino acid residues involved in H-bonding	No. of bumps	Amino acid residues involved in bumps
N1 WT	-6.44	2	Arg 152, Asn 294	18	Arg 118, 153, 224; Glu 119, 227, 277; Leu 134; Asp 151; Trp 178, 295; Ser 179, 246; Ile 222; Pro 245; Asn 247, 347; Ala 346; Tyr 406	-7.44	6	Arg 118, 152, 292, 371; Glu 119; Asp 151	8	Trp 178; Ile 222; Arg 224; Ser 246; Glu 276, 277; Asn 294; Tyr 406
N1 H275Y	-7.49	4	Asp 151; Arg 152; Ser 246	17	Glu 119, 227, 277; Leu 134; Arg 156, 224, 292; Trp 178; Ser 179; Asn 221, 247, 294; Ile 222; Gly 244; Pro 245; Tyr 347, 406	-7.98	7	Arg 118, 152, 292, 371; Glu 119; Tyr 347	9	Asp 151; Trp 178; Ile 222; Arg 224; Ser 246; Glu 276, 277; Asn 294; Tyr 406
N2 WT	-7.59	5	Arg 224, 292; Asn 294; His 347	17	Glu 119, 227, 276, 277; Leu 134; Asp 151; Arg 152; Trp 178, 295; Ser 179, 245, 247; Ile 222; Thr 225; Ala 246; Gly 346; Tyr 406	-8.57	6	Glu 119; Asp 151; Arg 152, 282, 371	10	Arg 118, 224; Trp 178; Ile 222; Ala 246; Glu 276, 277; Asn 294; His 347; Tyr 406
N2 E119V	-7.65	5	Arg 224, 292, 371; Asn 347	13	Asp 151; Arg 152; Trp 179; Ser 179; Ile 222; Leu 223; Glu 227, 276; Ala 246; Thr 247; Asn 294, 346	-8.20	10	Arg 118, 152, 292, 371; Asp 151; Trp 178; Glu 227; Tyr 406	6	Leu 134; Arg 156, 224; Ile 222; Glu 276, 277
N B	-7.60	4	Arg 115; Ala 244; Tyr 408	17	Arg 146, 149, 222, 291, 373; Asp 148; Trp 176, 407; Ser 177, 247, 248; Lys 219; Ile 220; Leu 221; Gly 242; Glu 275; His 438	-7.99	7	Arg 115, 149, 291, 373; Glu 116; Asp 148	7	Trp 176; Ile 220; Arg 222; Ala 244; Glu 274; Asn 293; Tyr 408

Table 4
Potency against influenza replication and cytotoxicity of compound **1i**

Compound	EC ₅₀ (μM)	CC ₅₀ (μM)	SI ^a
1i	0.20 ± 0.01	566 ± 89.5	2,830
Oseltamivir	0.03 ± 0.0023	321 ± 26	10,700

^a SI, selective index is determined by the ratio between CC₅₀ and EC₅₀ values.

for compound **1i** antiviral activity. Some of the amino acid residues required for the docking of compound **1i** are conserved, and changes in these residues could reduce virus fitness. These results indicate that the chemical structure of our synthesized oxoquinoline analogues are interesting prototypes for further development of novel anti-influenza drugs.

5. Experimental

5.1. Chemistry

5.1.1. Synthesis of ethyl-1-ethyl-7-azido-4-oxo-1,4-dihydroquinoline-3-carboxylate (**4b**)

The new compound **4b** was synthesized as described previously by us to obtain the derivative **4a**.²⁵ Reaction of 1-ethyl-3-carbomethoxy-7-amino-4-oxo-1,4-dihydroquinoline with nitrous acid (generated in situ from NaNO₃ and HCl) followed by the addition of sodium azide afforded the new compound **4b** at a yield of 84%. **4b**: 1-ethyl-3-carbomethoxy-7-azido-4-oxo-1,4-dihydroquinoline (84%) mp 143–145 °C; ¹H NMR (300.00 MHz, DMSO-*d*₆, internal standard: Me₄Si), δ 8.55 (s, 1H, H-2), 8.53 (d, 1H, *J* = 8.5 Hz, H-5), 7.15 (dd, 1H, *J* = 8.5; 1.8 Hz, H-6), 6.96 (d, 1H, *J* = 1.8 Hz, H-8), 4.40 (q, 2H, *J* = 7.1 Hz, NCH₂CH₃), 4.22 (q, 2H, *J* = 7.1 Hz, OCH₂CH₃), 1.54 (t, 3H, *J* = 7.1 Hz, NCH₂CH₃), and 1.42 (t, 3H, *J* = 7.1 Hz, OCH₂CH₃); ¹³C NMR (75.0 MHz, DMSO-*d*₆) δ

172.0 (C-4), 164.4 (CO₂CH₂CH₃), 149.2 (C-2), 144.1 (C-8a), 139.7 (C-6), 128.7 (C-4a), 125.3 (C-7), 116.2 (C-8), 110.4 (C-5), 106.6 (C-3), 59.7 (OCH₂CH₃), 47.8 (NCH₂CH₃), 14.2 (OCH₂CH₃), and 14.1 (NCH₂CH₃); HRMS (ESI) *m/z*: calcd for C₁₄H₁₄N₄O₃ [M+H]⁺ 287.1144, and found 287.1143.

5.1.2. Synthesis of ethyl 1-ethyl-(1,2,3-triazol-1'-yl)-4-oxo-1,4-dihydroquinoline-3-carboxylates (**1a–j**)

CuSO₄·5H₂O (17.5 mg, 0.07 mmol) and ascorbic acid (29.6 mg, 0.15 mmol) were added to a solution of azidoquinolone (**10a** or **10b**, 100 mg, 0.37 mmol) and the desired alkyne (0.55 mmol) in DMF (10.0 mL).

The resulting solution was stirred for 2 h (monitored by TLC) at 50 °C. After this time, the reaction mixture was poured into ice, leading to a yellow solid that was purified by flash column chromatography (CH₂Cl₂/EtOH as the gradient). **1a**: ethyl 1-ethyl-6-[4'-(2''-hydroxypropan-2''-yl)-1*H* -1,2,3-triazol-1'-yl]-4-oxo-1,4-dihydroquinoline-3-carboxylate (88%), mp 175–177 °C; ¹H NMR (300.00 MHz, DMSO-*d*₆, internal standard: Me₄Si), δ 8.77 (s, 1H, H-5'), 8.75 (s, 1H, H-2), 8.66 (d, 1H, *J* = 2.4 Hz, H-5), 8.33 (dd, 1H, *J* = 9.1; 2.4; H-7), 8.06 (d, 1H, *J* = 9.1; H-8), 5.26 (s, 1H, C(CH₃)₂OH), 4.48 (q, 2H, *J* = 6.8 Hz, OCH₂CH₃), 4.25 (q, 2H, *J* = 7.0 Hz, NCH₂CH₃), 1.56 (s, 6H, C(CH₃)₂OH), 1.40 (t, 3H, *J* = 6.8 Hz, OCH₂CH₃), and 1.30 (t, 3H, *J* = 7.0 Hz, NCH₂CH₃); ¹³C NMR (75.0 MHz, DMSO-*d*₆) δ 172.2 (C-4), 164.3 (CO₂CH₂CH₃), 157.0 (C-4'), 149.2 (C-2), 137.9 (C-8a), 133.4 (C-6), 129.0 (C-4a), 124.2 (C-7), 119.0 (C-5'), 119.3 (C-8), 116.6 (C-5), 110.3 (C-3), 66.9 (C(CH₃)₂OH), 59.8 (NCH₂CH₃), 48.1 (OCH₂CH₃), 30.4 (C(CH₃)₂OH), 14.3 (OCH₂CH₃), and 14.2 (NCH₂CH₃); ESI-FTICRMS: *m/z* calcd for C₁₉H₂₂N₄O₄ [M+H]⁺ 371.1873, found 371.1870; **1b**: ethyl 1-ethyl-7-[4'-(2''-hydroxypropan-2''-yl)-1*H* -1,2,3-triazol-1'-yl]-4-oxo-1,4-dihydroquinoline-3-carboxylate (85%), mp 179–181 °C; ¹H NMR (300.00 MHz, DMSO-*d*₆, internal standard: Me₄Si) δ 8.92 (s, 1H, H-5'), 8.75

(s, 1H, H-2), 8.40 (d, 1H, $J = 8.8$ Hz, H-5), 8.07 (dd, 1H, $J = 8.8$; 1.7; H-6), 8.20 (d, 1H, $J = 1.7$; H-8), 4.52 (q, 2H, $J = 7.1$ Hz, OCH_2CH_3), 4.24 (q, 2H, $J = 7.1$ Hz, NCH_2CH_3), 1.56 (s, 6H, $\text{C}(\text{CH}_3)_2\text{OH}$), 1.41 (t, 3H, $J = 7.1$ Hz, OCH_2CH_3), and 1.30 (t, 3H, $J = 7.1$ Hz, NCH_2CH_3); ^{13}C NMR (75.0 MHz, $\text{DMSO}-d_6$) δ 172.2 (C-4), 164.3 ($\text{CO}_2\text{CH}_2\text{CH}_3$), 157.3 (C-4'), 149.7 (C-2), 139.7 (C-8a), 139.5 (C-7), 127.4 (C-4a), 128.7 (C-5), 119.4 (C-5'), 116.3 (C-6), 110.8 (C-3), 107.3 (C-8), 67.0 ($\text{C}(\text{CH}_3)_2\text{OH}$), 59.8 (NCH_2CH_3), 48.0 (OCH_2CH_3), 30.5 ($\text{C}(\text{CH}_3)_2\text{OH}$), 14.3 (OCH_2CH_3), and 14.2 (NCH_2CH_3); ESI-FTICRMS: m/z calcd for $\text{C}_{19}\text{H}_{22}\text{N}_4\text{O}_4$ [$\text{M}+\text{H}$] 371.1873, found 371.1876; **1c**: ethyl 1-ethyl-6-[4'-(1''-hydroxycyclohexyl)-1H -1,2,3-triazol-1'-yl]-4-oxo-1,4-dihydroquinoline-3-carboxylate (83%), mp 228–230 °C; ^1H NMR (300.00 MHz, $\text{DMSO}-d_6$) δ 8.77 (s, 1H, H-5'), 8.74 (s, 1H, H-2), 8.66 (d, 1H, $J = 2.4$ Hz, H-5), 8.32 (dd, 1H, $J = 9.2$; 2.4 Hz, H-7), 8.05 (d, 1H, $J = 9.2$ Hz, H-8), 4.48 (q, 2H, $J = 6.8$ Hz, OCH_2CH_3), 4.25 (q, 2H, $J = 7.1$ Hz, NCH_2CH_3), 2.03–1.48 (m, 10H, H-2'' to H-6''), 1.40 (t, 3H, $J = 6.8$ Hz, OCH_2CH_3), and 1.30 (t, 3H, $J = 7.1$ Hz, NCH_2CH_3); ^{13}C NMR (75.0 MHz, $\text{DMSO}-d_6$) δ 172.1 (C-4), 164.3 ($\text{CO}_2\text{CH}_2\text{CH}_3$), 156.8 (C-4'), 149.1 (C-2), 137.9 (C-8a), 133.4 (C-6), 124.1 (C-7), 120.0 (C-4a), 119.4 (C-5'), 119.3 (C-8), 116.6 (C-5), 110.3 (C-3), 67.8 (C-1''), 59.7 (NCH_2CH_3), 48.1 (OCH_2CH_3), 37.5 (C-2'' and C-6''), 25.1 (C-4''), 21.6 (C-3'' and C-5''), 14.3 (OCH_2CH_3), and 14.2 (NCH_2CH_3); ESI-FTICRMS: m/z calcd for $\text{C}_{22}\text{H}_{26}\text{N}_4\text{O}_4$ [$\text{M}+\text{H}$] 411.2227, found 411.2222; **1d**: ethyl 1-ethyl-7-[4'-(1''-hydroxycyclohexyl)-1H -1,2,3-triazol-1'-yl]-4-oxo-1,4-dihydroquinoline-3-carboxylate (79%) mp 105–107 °C; ^1H NMR (300.00 MHz, $\text{DMSO}-d_6$, internal standard: Me_4Si) δ 8.93 (s, 1H, H-5'), 8.74 (s, 1H, H-2), 8.41 (d, 1H, $J = 8.8$ Hz, H-5), 8.07 (dd, 1H, $J = 8.8$; 1.8 Hz, H-6), 8.20 (d, 1H, $J = 1.8$ Hz, H-8), 4.52 (q, 2H, $J = 7.1$ Hz, OCH_2CH_3), 4.25 (q, 2H, $J = 7.0$ Hz, NCH_2CH_3), 2.02–1.49 (m, 10H, H-2'' to H-6''), 1.46 (t, 3H, $J = 7.1$ Hz, OCH_2CH_3), and 1.30 (t, 3H, $J = 7.1$ Hz, NCH_2CH_3); ^{13}C NMR (75.0 MHz, $\text{DMSO}-d_6$) δ 172.0 (C-4), 164.2 ($\text{CO}_2\text{CH}_2\text{CH}_3$), 157.1 (C-4'), 149.4 (C-2), 139.6 (C-7), 139.4 (C-8a), 128.5 (C-5), 127.2 (C-4a), 119.6 (C-5'), 116.0 (C-6), 110.1 (C-3), 107.1 (C-8), 67.9 (C-1''), 59.5 (NCH_2CH_3), 47.7 (OCH_2CH_3), 37.3 (C-2'' and C-6''), 24.8 (C-4''), 21.2 (C-3'' and C-5''), 14.0 (OCH_2CH_3), and 13.9 (NCH_2CH_3); ESI-FTICRMS: m/z calcd for $\text{C}_{22}\text{H}_{26}\text{N}_4\text{O}_4$ [$\text{M}+\text{H}$] 411.2227, found 411.2226; **1e**: ethyl 1-ethyl-6-(4'-phenyl-1H -1,2,3-triazol-1'-yl)-4-oxo-1,4-dihydroquinoline-3-carboxylate (97%), mp 237–239 °C; ^1H NMR (300.00 MHz, $\text{DMSO}-d_6$, internal standard: Me_4Si) δ 9.46 (s, 1H, H-5'), 8.74 (s, 1H, H-2), 8.73 (d, 1H, $J = 2.7$ Hz, H-5), 8.37 (dd, 1H, $J = 9.1$; 2.7 Hz, H-7), 8.10 (d, 1H, $J = 9.1$ Hz, H-8), 7.99 (d, 2H, $J = 7.1$ Hz, H-2'' and H-6''), 7.51 (t, 2H, $J = 7.3$ Hz, H-3'' and H-5''), 7.40 (t, 1H, $J = 7.1$ Hz, H-4''), 4.48 (q, 2H, $J = 7.1$ Hz, OCH_2CH_3), 4.27 (q, 2H, $J = 7.1$ Hz, NCH_2CH_3), 1.44 (t, 3H, $J = 7.1$ Hz, OCH_2CH_3), and 1.32 (t, 3H, $J = 7.1$ Hz, NCH_2CH_3); ^{13}C NMR (75.0 MHz, $\text{DMSO}-d_6$) δ 172.1 (C-4), 164.2 ($\text{CO}_2\text{CH}_2\text{CH}_3$), 149.0 (C-2), 147.4 (C-4'), 138.1 (C-8a), 133.1 (C-6), 131.5 (C-1''), 130.0 (C-4a), 128.7 (C-3'' and C-5''), 128.1 (C-4''), 125.2 (C-2'' and C-6''), 124.1 (C-7), 119.3 (C-8), 116.7 (C-5), 115.0 (C-5'), 110.4 (C-3), 59.6 (NCH_2CH_3), 48.0 (OCH_2CH_3), 14.2 (OCH_2CH_3), and 14.1 (NCH_2CH_3); ESI-FTICRMS: m/z calcd for $\text{C}_{22}\text{H}_{20}\text{N}_4\text{O}_3$ [$\text{M}+\text{H}$] 389.1535, found 389.1532; **1f**: ethyl 1-ethyl-7-(4'-phenyl-1H -1,2,3-triazol-1'-yl)-4-oxo-1,4-dihydroquinoline-3-carboxylate (93%) mp 127–129 °C; ^1H NMR (300.00 MHz, $\text{DMSO}-d_6$, internal standard: Me_4Si) δ 9.52 (s, 1H, H-5'), 8.76 (s, 1H, H-2), 8.46 (d, 1H, $J = 8.7$ Hz, H-5), 8.09 (dd, 1H, $J = 8.7$; 1.6 Hz, H-6), 8.26 (d, 1H, $J = 1.6$ Hz, H-8), 7.97 (dd, 2H, $J = 8.2$; 1.2 Hz, H-2'' and H-6''), 7.54 (t, 2H, $J = 7.2$ Hz, H-3'' and H-5''), 7.43 (t, 1H, $J = 7.2$ Hz, H-4''), 4.52 (q, 2H, $J = 7.0$ Hz, OCH_2CH_3), 4.25 (q, 2H, $J = 7.0$ Hz, NCH_2CH_3), 1.46 (t, 3H, $J = 7.0$ Hz, OCH_2CH_3), and 1.31 (t, 3H, $J = 7.0$ Hz, NCH_2CH_3); ^{13}C NMR (75.0 MHz, $\text{DMSO}-d_6$) δ 171.9 (C-4), 164.0 ($\text{CO}_2\text{CH}_2\text{CH}_3$), 149.4 (C-2), 147.3 (C-4'), 139.2 (C-8a and C-7), 129.3 (C-1''), 128.8 (C-3'' and C-5''), 128.3 (C-4''), 127.4 (C-4a), 125.1 (C-2'' and C-6''), 128.7 (C-5), 119.9 (C-5'), 116.2 (C-6), 108.1 (C-3), 107.5 (C-8), 59.6 (NCH_2CH_3), 47.8

(OCH_2CH_3), 14.0 (OCH_2CH_3), and 13.9 (NCH_2CH_3); ESI-FTICRMS: m/z calcd for $\text{C}_{22}\text{H}_{20}\text{N}_4\text{O}_3$ [$\text{M}+\text{H}$] 389.1535, found 389.1538; **1g**: ethyl 1-ethyl-6-[4'-(hydroxymethyl)-1H -1,2,3-triazol-1'-yl]-4-oxo-1,4-dihydroquinoline-3-carboxylate (95%) mp 220–221 °C; ^1H NMR (300.00 MHz, $\text{DMSO}-d_6$, internal standard: Me_4Si) δ 8.85 (s, 1H, H-5'), 8.75 (s, 1H, H-2), 8.66 (d, 1H, $J = 2.7$ Hz, H-5), 8.32 (dd, 1H, $J = 9.3$; 2.7, H-7), 8.07 (d, 1H, $J = 9.3$; H-8), 5.35 (t, 1H, $J = 5.5$ Hz, CH_2OH), 4.63 (d, 2H, $J = 5.5$ Hz, CH_2OH), 4.48 (q, 2H, $J = 7.1$ Hz, OCH_2CH_3), 4.25 (q, 2H, $J = 7.3$ Hz, NCH_2CH_3), 1.40 (t, 3H, $J = 7.1$ Hz, OCH_2CH_3), and 1.30 (t, 3H, $J = 7.3$ Hz, NCH_2CH_3); ^{13}C NMR (75.0 MHz, $\text{DMSO}-d_6$) δ 172.2 (C-4), 164.4 ($\text{CO}_2\text{CH}_2\text{CH}_3$), 149.3 (C-4'), 149.2 (C-2), 138.0 (C-8a), 133.4 (C-6), 129.0 (C-4a), 124.3 (C-7), 121.2 (C-5'), 119.4 (C-8), 116.8 (C-5), 110.3 (C-3), 59.8 (NCH_2CH_3), 54.9 (CH_2OH), 48.2 (OCH_2CH_3), 14.4 (OCH_2CH_3), and 14.3 (NCH_2CH_3); ESI-FTICRMS: m/z calcd for $\text{C}_{17}\text{H}_{18}\text{N}_4\text{O}_4$ [$\text{M}+\text{H}$] 343.1328, found 343.1324; **1h**: ethyl 1-ethyl-7-[4'-(hydroxymethyl)-1H -1,2,3-triazol-1'-yl]-4-oxo-1,4-dihydroquinoline-3-carboxylate (90%) mp 223–225 °C; ^1H NMR (300.00 MHz, $\text{DMSO}-d_6$, internal standard: Me_4Si) δ 9.00 (s, 1H, H-5'), 8.75 (s, 1H, H-2), 8.41 (d, 1H, $J = 8.6$ Hz, H-5), 8.21 (d, 1H, $J = 1.7$; H-8), 8.07 (dd, 1H, $J = 8.6$; 1.7, H-6), 4.66 (s, 1H, CH_2OH), 4.51 (q, 2H, $J = 7.1$ Hz, OCH_2CH_3), 4.25 (q, 2H, $J = 7.1$ Hz, NCH_2CH_3), 1.42 (t, 3H, $J = 7.1$ Hz, OCH_2CH_3), and 1.30 (t, 3H, $J = 7.1$ Hz, NCH_2CH_3); ^{13}C NMR (75.0 MHz, $\text{DMSO}-d_6$) δ 172.0 (C-4), 164.4 ($\text{CO}_2\text{CH}_2\text{CH}_3$), 149.5 (C-4'), 149.7 (C-2), 139.5 (C-8a), 128.8 (C-5), 127.4 (C-4a), 124.3 (C-7), 121.6 (C-5'), 116.3 (C-6), 110.8 (C-3), 107.5 (C-8), 59.8 (NCH_2CH_3), 54.9 (CH_2OH), 48.0 (OCH_2CH_3), 14.3 (OCH_2CH_3), and 14.2 (NCH_2CH_3); ESI-FTICRMS: m/z calcd for $\text{C}_{17}\text{H}_{18}\text{N}_4\text{O}_4$ [$\text{M}+\text{H}$] 343.1328, found 343.1326; **1i**: ethyl 1-ethyl-6-(4'-cyclohexenyl-1H -1,2,3-triazol-1'-yl)-4-oxo-1,4-dihydroquinoline-3-carboxylate (98%) mp 230–231 °C; ^1H NMR (300.00 MHz, $\text{DMSO}-d_6$, internal standard: Me_4Si) δ 8.94 (s, 1H, H-5'), 8.73 (s, 1H, H-2), 8.67 (d, 1H, $J = 2.5$ Hz, H-5), 8.30 (dd, 1H, $J = 9.1$; 2.5 Hz, H-7), 8.06 (d, 1H, $J = 9.1$ Hz, H-8), 6.58 (t, 1H, $J = 3.6$ Hz, H-2''), 4.47 (q, 2H, $J = 7.0$ Hz, OCH_2CH_3), 4.26 (q, 2H, $J = 7.1$ Hz, NCH_2CH_3), 1.96–1.74 (m, 8H, H-3'' to H-6''), 1.42 (t, 3H, $J = 7.0$ Hz, OCH_2CH_3), and 1.31 (t, 3H, $J = 7.1$ Hz, NCH_2CH_3); ^{13}C NMR (75.0 MHz, $\text{DMSO}-d_6$) δ 172.2 (C-4), 164.2 ($\text{CO}_2\text{CH}_2\text{CH}_3$), 149.0 (C-2), 149.1 (C-4'), 137.9 (C-8a), 133.3 (C-6), 129.0 (C-4a), 127.0 (C-1''), 124.5 (C-2''), 124.0 (C-7), 119.3 (C-8), 118.0 (C-5'), 116.5 (C-5), 110.3 (C-3), 59.7 (NCH_2CH_3), 48.1 (OCH_2CH_3), 24.6 (C-6''), 25.7 (C-3''), 21.9 (C-4''), 21.7 (C-5''), 14.3 (OCH_2CH_3), and 14.2 (NCH_2CH_3); ESI-FTICRMS: m/z calcd for $\text{C}_{22}\text{H}_{24}\text{N}_4\text{O}_3$ [$\text{M}+\text{H}$] 393.1758, found 393.1754; **1j**: ethyl 1-ethyl-7-(4'-cyclohexenyl-1H -1,2,3-triazol-1'-yl)-4-oxo-1,4-dihydroquinoline-3-carboxylate (95%), mp 235–237 °C; ^1H NMR (300.00 MHz, $\text{DMSO}-d_6$, internal standard: Me_4Si) δ 9.02 (s, 1H, H-5'), 8.75 (s, 1H, H-2), 8.41 (d, 1H, $J = 8.7$ Hz, H-5), 8.17 (d, 1H, $J = 1.6$ Hz, H-8), 8.05 (dd, 1H, $J = 8.7$; 1.6 Hz, H-6), 6.59 (t, 1H, $J = 3.6$ Hz, H-2''), 4.48 (q, 2H, $J = 6.8$ Hz, NCH_2CH_3), 4.25 (q, 2H, $J = 7.0$ Hz, OCH_2CH_3), 2.44–2.42 (m, 2H, H-3'' or H-6''), 2.22–2.10 (m, 2H, H-3'' or H-6''), 1.80–1.72 (m, 2H, H-4'' or H-5''), 1.67–1.64 (m, 2H, H-4'' or H-5''), 1.40 (t, 3H, $J = 6.8$ Hz, NCH_2CH_3), and 1.30 (t, 3H, $J = 7.0$ Hz, NCH_2CH_3); ^{13}C NMR (75.0 MHz, $\text{DMSO}-d_6$) δ 172.3 (C-4), 164.5 ($\text{CO}_2\text{CH}_2\text{CH}_3$), 149.6 (C-4'), 149.4 (C-2), 139.8 (C-7 and C-8a), 128.6 (C-5), 127.8 (C-4a), 127.2 (C-1''), 124.7 (C-2''), 117.7 (C-5'), 116.0 (C-6), 110.2 (C-3), 107.1 (C-8), 59.7 (NCH_2CH_3), 47.8 (OCH_2CH_3), 25.5 (C-6''), 24.4 (C-3''), 21.6 (C-4''), 21.5 (C-5''), 14.1 (OCH_2CH_3), and 14.0 (NCH_2CH_3); ESI-FTICRMS: m/z calcd for $\text{C}_{22}\text{H}_{24}\text{N}_4\text{O}_3$ [$\text{M}+\text{H}$] 393.1758, found 393.1755.

5.2. Cells and viruses

Madin-Darby canine kidney epithelial cells (MDCKs) were cultured in Dulbecco's Modified Eagle Medium (DMEM; Life Technologies, Grand Island, NY) supplemented with 10% fetal bovine serum and antibiotics (100 U/mL penicillin and 100 $\mu\text{g}/\text{mL}$

streptomycin) at 37 °C and 5% CO₂. Both wild-type and NAI-resistant influenza A and B virus strains (Table S3) were propagated in MDCKs and stored at –70 °C. The influenza strains displayed in Table S3 were kindly donated by Dr. Larisa V. Gubareva and Dr. Alexander I. Klimov from the Centers for Disease Control (CDC), Atlanta, to the Brazilian National Influenza Center (NIC) at FIOCRUZ, Rio de Janeiro. These viruses are reference strains used for laboratory-based surveillance to monitor the antiviral susceptibility of circulating influenza viruses to NAIs.

5.2.1. Cytotoxicity assay

Monolayers of 2×10^4 MDCKs in 96-well culture plates were incubated with the compounds at different concentrations for 72 h. Then, 2,3-bis-(2-methoxy-4-nitro-5-sulphophenyl)-2H-tetrazolium-5-carboxanilide (XTT) at 5 mg/mL was added to the DMEM in the presence of 0.01% *N*-methyl-dibenzopirazin methyl sulfate (PMS). After incubation for 4 h at 37 °C, the plates were read in a spectrophotometer at 492 nm and 620 nm.²⁹ The 50% cytotoxic concentration (CC₅₀) was calculated by linear regression analysis of the dose–response curves generated from the data.

5.2.2. Yield reduction assay

Monolayers of MDCK cells (2×10^5 cell/well) in 24-well plates were infected with influenza at an MOI of 0.05 for 1 h at 37 °C. Cells were washed to remove residual viruses and various concentrations of the compounds were added. After 24 h, viruses in the supernatant were harvested and titrated by end-point 50% cell culture infective dose (TCID₅₀/mL) using MDCK cells. For comparison, the reference compound OST carboxylate (kindly donated by Hoffman-La Roche Inc., Basel, Switzerland) was used as a positive control. Linear regression of the dose–response curve was performed to determine the 50% inhibitory effect on viral replication (EC₅₀) for the tested and reference compounds.

5.2.3. Influenza titration

MDCKs plated in 96-well plates (5×10^4 cells/well) were infected with serial 10-fold dilutions of the supernatants from the yield-reduction assays described above for 1 h at 37 °C and 5% CO₂. Then, viruses were washed out and the cells were incubated for 72 h. After this period of time, influenza-induced cytopathic effects (CPE) were scored by TCID₅₀.^{30,31}

5.2.4. NA inhibition assay

To evaluate the ability of the compounds to inhibit the NA activity of the influenza strains described in Table S1, we performed cell-free based assays using the NA-Starkit (Life Technologies, CA) according to the manufacturer's instructions. Briefly, the NA activity of the different influenza virus strains was titrated. Next, the NA activity was measured in the presence of different concentrations of the compounds to determine the enzyme inhibition. The concentration able to inhibit 50% of influenza's NA activity (IC₅₀) was calculated using non-linear regression. For comparison, every assay was performed with OST carboxylate as a positive control.

5.3. In silico docking

Docking of the compound **1i** or OST with different NAs (Table S4) was performed using the ArgusLab 4.0.1 software (Planaria Software LLC).³² The crystal structures of WT and OST-resistant NAs were obtained from the Protein Data Bank (PDB, www.rcsb.org).³³ PDB accession numbers and the degree of resolution of the X-ray crystals are shown in Table S2. We selected these files because they already have an OST molecule bound in the crystal structure of the NA. To our knowledge, no OST-resistant influenza B NA structure is deposited in the PDB. Before docking, the structures of the proteins were cleaned by removing the water

molecules and external ligands, with the exception of OST. The modified structure was saved in the .pdb format to be used in all docking studies. The structure of compound **1i** was designed using Accelrys Draw 4.1 software (Accelrys, Inc.) and improved using Accelrys® Discovery Studio 3.5 software to add hydrogens and optimize the compound geometry (UFF Molecular Mechanics method).³⁴ The optimized **1i** molecule file was saved in .mol format for further docking studies. The docking between the ligand **1i** and each NA enzyme isoform was performed using the 'Dock a Ligand' option in the Arguslab software. The area occupied by amino acid residues involved in the docking of OST was considered to be the center of the actual **1i** bind site (Table S2). A spacing of 0.4 Å between the grid points was used and the ligand was assumed to be flexible and the protein rigid. A maximum of 150 poses were allowed in the analysis, and each docking run was repeated three times to obtain the best results. 'ArgusDock' and 'Dock' were chosen as the docking engine for the simulations and calculation type, respectively. Displays of the 2D interactions between compound **1i** and different NAs were obtained with Accelrys® Discovery Studio 3.5 software.³⁵ OST was docked over the original reference compound found in these protein X-ray structures as a control. Poses with lower free-energy and with differences smaller than 3 Å between the two docked OST structures were considered to be reliable.

5.3.1. Alignment of genetically diverse neuraminidases

To compare the relevant residues found in the docking analysis with their equivalents on the sequenced NA isoforms found in nature, we created alignments using Mega 6.06 software. DNA sequences were aligned by Clustal W (1.6), and amino acid residues were predicted. We have chosen to align the complete genome segment of influenza A NA isoforms N1–N9 (NCBI codes and influenza strains are listed in Table S4) and analyzed specific regions containing the amino acid residues involved in the **1i** and NA interactions.

5.4. Statistical analyses

The dose–response curves used to calculate the IC₅₀, EC₅₀ and CC₅₀ values were generated by Excel for Windows. All of the experiments were performed at least three times, and the results are displayed as mean ± standard error of the mean (SEM).

Acknowledgments

We thank the Conselho Nacional de Desenvolvimento Científico e Tecnológico (CNPq), Coordenação de Aperfeiçoamento de Pessoal Docente (CAPES) and Fundação de Amparo à Pesquisa do Estado do Rio de Janeiro (FAPERJ) for financial support and fellowships.

Supplementary data

Supplementary data associated with this article can be found, in the online version, at <http://dx.doi.org/10.1016/j.bmc.2015.11.028>.

References and notes

1. Damjanovic, D.; Small, C. L.; Jeyanathan, M.; Jeyanathan, M.; McCormick, S.; Xing, Z. *Clin. Immunol.* **2012**, *144*, 57.
2. Murphy, B. R.; Webster, R. G. *Orthomyxoviruses*, 3rd ed.; Lippincott-Raven: Philadelphia, 1996.
3. Tang, J. W.; Shetty, N.; Lam, T. T.; Hon, K. L. *Infect. Dis. Clin. North Am.* **2010**, *24*, 603.
4. Kollerova, E.; Betakova, T. *Acta Virol.* **2006**, *50*, 7.
5. Das, K.; Aramini, J. M.; Ma, L. C.; Krug, R. M.; Arnold, E. *Nat. Struct. Mol. Biol.* **2010**, *17*, 530.

6. Grohskopf, L. A.; Olsen, S. J.; Sokolow, L. Z.; Bresee, J. S.; Cox, N. J.; Broder, K. R.; Karron, R. A.; Walter, E. B. C. f. D. C. a Prevention *MMWR Morb. Mortal. Wkly. Rep.* **2014**, *63*, 691.
7. Fiore, A. E.; Fry, A.; Shay, D.; Gubareva, L.; Bresee, J. S.; Uyeki, T. M. *MMWR Recomm. Rep.* **2011**, *60*, 1.
8. Manz, B.; Schwemmler, M.; Brunotte, L. *J. Virol.* **2013**, *87*, 7200.
9. WHO *Wkly. Epidemiol. Rec.* **2013**, *88*, 437.
10. Muthuri, S. G.; Myles, P. R.; Venkatesan, S.; Leonardi-Bee, J.; Nguyen-Van-Tam, J. S. *J. Infect. Dis.* **2013**, *207*, 553.
11. Balicer, R. D.; Huerta, M.; Davidovitch, N.; Grotto, I. *Emerg. Infect. Dis.* **2005**, *11*, 1280.
12. Patel, A.; Gorman, S. E. *Clin. Pharmacol. Ther.* **2009**, *86*, 241.
13. Hurt, A. C. *Curr. Opin. Virol.* **2014**, *8C*, 22.
14. Jefferson, T.; Jones, M.; Doshi, P.; Spencer, E. A.; Onakpoya, I.; Heneghan, C. J. *BMJ* **2014**, *348*, g2545.
15. Fry, A. M.; Gubareva, L. V. *J. Infect. Dis.* **2012**, *206*, 145.
16. Hurt, A. C.; Hardie, K.; Wilson, N. J.; Deng, Y. M.; Osbourn, M.; Leang, S. K.; Lee, R. T.; Iannello, P.; Gehrig, N.; Shaw, R.; Wark, P.; Caldwell, N.; Givney, R. C.; Xue, L.; Maurer-Stroh, S.; Dwyer, D. E.; Wang, B.; Smith, D. W.; Levy, A.; Booy, R.; Dixit, R.; Merritt, T.; Kelso, A.; Dalton, C.; Durrheim, D.; Barr, I. G. *J. Infect. Dis.* **2012**, *206*, 148.
17. Souza, T. M. L.; Rodrigues, D. Q.; Ferreira, V. F.; Marques, I. P.; Santos, F. C.; Cunha, A. C.; Souza, M. C. B. V.; Frugulhetti, I. C. P. P.; Bou-Habib, D. C.; Fontes, C. F. L. *Curr. HIV Res.* **2009**, *7*, 327.
18. Wang, Z.; Wu, B.; Kuhen, K. L.; Bursulaya, B.; Nguyen, T. N.; Nguyen, D. G.; He, Y. *Bioorg. Med. Chem. Lett.* **2006**, *16*, 4174.
19. Duffin, G. F.; Kendall, J. D. *J. Chem. Soc.* **1948**, *70*, 893.
20. Kumar, D. V.; Rai, R.; Brameld, K. A.; Somoza, J. R.; Rajagopalan, R.; Janc, J. W.; Xia, Y. M.; Ton, T. L.; Shaghafi, M. B.; Hu, H.; Lehoux, I.; To, N.; Young, W. B.; Green, M. J. *Bioorg. Med. Chem. Lett.* **2011**, *21*, 82.
21. Wittine, K.; Stipković Babić, M.; Makuc, D.; Plavec, J.; Kraljević Pavelić, S.; Sedić, M.; Pavelić, K.; Leyssen, P.; Neyts, J.; Balzarini, J.; Mintas, M. *Bioorg. Med. Chem.* **2012**, *20*, 3675.
22. Li, J.; Zheng, M.; Tang, W.; He, P. L.; Zhu, W.; Li, T.; Zuo, J. P.; Liu, H.; Jiang, H. *Bioorg. Med. Chem. Lett.* **2006**, *16*, 5009.
23. Glowacka, I. E.; Balzarini, J.; Andrei, G.; Snoeck, R.; Schols, D.; Piotrowska, D. G. *Bioorg. Med. Chem.* **2014**, *22*, 3629.
24. Ruxer, J. M.; Lachoux, C.; Ousset, J. B.; Torregrosa, J. L.; Mattioda, G. *J. Heterocycl. Chem.* **1994**, *31*, 409.
25. Abreu, P. A.; da Silva, V. A. G. G.; Santos, F. C.; Castro, H. C.; Riscado, C. S.; Souza, M. T.; Ribeiro, C. P.; Barbosa, J. E.; dos Santos, C. C. C.; Rodrigues, C. R.; Lione, V.; Correa, B. A. M.; Cunha, A. C.; Ferreira, V. F.; Souza, M. C. B. V.; Paixão, I. C. N. P. *Curr. Microbiol.* **2011**, *62*, 1349.
26. Webster, R. G.; Govorkova, E. A. *Ann. N. Y. Acad. Sci.* **2014**, *1323*, 115.
27. von Itzstein, M.; Wu, W. Y.; Kok, G. B.; Pegg, M. S.; Dyason, J. C.; Jin, B.; Van Phan, T.; Smythe, M. L.; White, H. F.; Oliver, S. W. *Nature* **1993**, *363*, 418.
28. Aoki, F. Y.; Boivin, G.; Roberts, N. *Antiviral Ther.* **2007**, *12*, 603.
29. Scudiero, D. A.; Shoemaker, R. H.; Paull, K. D.; Monks, A.; Tierney, S.; Nofziger, T. H.; Currens, M. J.; Seniff, D.; Boyd, M. R. *Cancer Res.* **1988**, *48*, 4827.
30. Reed, L. J.; Muench, H. *Am. J. Epidemiol.* **1938**, *27*, 493.
31. WHO; CDC. Serological Diagnosis of Influenza by Microneutralization Assay; 2010.
32. Joy, S.; Nair, P. S.; Hariharan, R.; Pillai, M. R. *In Silico Biol.* **2006**, *6*, 601.
33. Bernstein, F. C.; Koetzle, T. F.; Williams, G. J.; Meyer, E. F.; Brice, M. D.; Rodgers, J. R.; Kennard, O.; Shimanouchi, T.; Tasumi, M. *Arch. Biochem. Biophys.* **1978**, *185*, 584.
34. Rappe, A. K.; Casewit, C. J.; Colwell, K. S.; Goddard, W. A. I.; Skiff, W. M. *J. Am. Chem. Soc.* **1992**, *114*, 10024.
35. Hussain Basha, S.; Prasad, R. N. *BMC Res. Notes* **2012**, *5*, 105.